Effect of substrate roughness, chemical composition, and native oxide crystallinity on the orientation of self-assembled GaN nanowires on Ti foils

G Calabrese[1,*], S V Pettersen[2], C Pfüller[1], M Ramsteiner[1], J K Grepstad[2], O Brandt[1], L Geelhaar[1], S Fernández-Garrido[1]

[1]Paul-Drude-Institut für Festkörperelektronik, Hausvogteiplatz 5–7, 10117 Berlin, Germany

[2]Department of Electronics and Telecommunications, NTNU—Norwegian University of Science and Technology, Trondheim 7491, Norway

E-mail: *calabrese@pdi-berlin.de

Abstract. We report on plasma-assisted molecular beam epitaxial growth of almost randomly oriented, uniformly tilted, and vertically aligned self-assembled GaN nanowires, respectively, on different types of polycrystalline Ti foils. The nanowire orientation, which is affected by an in-situ treatment of the foil surface before nanowire growth, depends on the crystallinity of the native oxide. Direct growth on the as-received foils results in the formation of ensembles of nearly randomly oriented nanowires due to the strong roughening of the surface induced by chemical reactions between the impinging elements and Ti. Surface nitridation preceding the nanowire growth is found to reduce this roughening by transformation of the uppermost layers into TiN and TiO_xN_y species. These compounds are more stable against chemical reactions and facilitate the growth of ensembles of uniformly oriented GaN nanowires within the individual grains of the polycrystalline Ti foils. If an amorphous oxide layer is present at the foil surface, vertically oriented nanowires are obtained all across the substrate because this layer blocks the transfering of the epitaxial information from the underlying grains. The control of nanowire orientation and the understanding behind the achievement of vertically oriented nanowires obtained in this study represent an important step towards the realization of GaN nanowire-based bendable devices on polycrystalline metal foils.

Submitted to: *Nanotechnology*

1. Introduction

Semiconducting nanowires (NWs) synthesized on metallic substrates have recently emerged as an interesting materials combination for fabrication of solid-state devices with novel and/or improved functionalities.[1–10] This hybrid material system benefits from the excellent structural quality of the semiconducting nanowires[11, 12] and the optical reflectivity as well as high thermal and electrical conductivity of the metallic substrate. So far, most efforts in this field were devoted to the integration of semiconducting NW ensembles on metallic films sputter-deposited on various substrates. Using this approach, different materials systems were investigated, such as Ge and Si NWs on Ag, Al, Au, Cr, Cu and Ni, [13] ZnO NWs on Au-coated glass,[14] Si and Al_2O_3,[15] and GaAs NWs on Pt and Ti.[16] Group-III nitride NWs were reported on sputter-deposited films of both Ti and Mo[1, 3, 4, 7–10], and NW-based light-emitting diodes (LEDs) were also demonstrated on these substrates.[3, 4, 7–9] While sputtered metal films offer significant advantages over conventional substrates for crystal growth, metal foils represent a more versatile kind of substrate. Besides the benefits inherent to a metallic substrate, metal foils can be exploited for fabrication of flexible electronic and photonic devices. In addition, the use of polycrystalline and large area metal foils as substrates might also lead to an increased throughput and a significant cost reduction. Direct growth of semiconducting NW ensembles on metal foils was demonstrated for Si on stainless steel, [17] CdS on Al [18] and Ag, [19] ZnO on Zn [20], and Ge on Au-coated Al foils.[21] In the case of group III-nitrides, GaN and (Al,Ga)N NWs were demonstrated on flexible Ti and Ta metal foils, [5, 6] while InN NWs were reported on brass foil substrates.[22] On Ta foils, GaN NW-based LEDs have also been recently demonstrated.[6] In a previous work we found that the structural and optical quality of self-assembled GaN NW ensembles grown on a Ti foil are comparable to those of similar structures grown on Si.[5] Moreover, the NW ensembles grown on the Ti foil were mechanically stable against bending of the substrate, hence holding great promise for the realization of GaN-based flexible devices.[5]

For many applications, vertical NW ensembles are highly desirable or even required. However, for NWs grown on metal foils a broad distribution of tilt angles with respect to the substrate normal is commonly observed [6, 17, 22]. For the case of GaN NWs grown on foils of Ti and Ta, this phenomenon was attributed to an epitaxial relation between the NWs and the individual grains of the polycrystalline metal foil.[6] As discussed in Ref. 6, the tilted growth of the NWs on different types of metal foils (Ti and Ta) complicates the subsequent processing of NW-based LEDs, which so far show higher leakage currents and reduced electroluminescence intensities compared to devices fabricated from NWs

grown on crystalline Si substrates. In striking contrast to these results, we have obtained vertically oriented GaN NWs on a polycrystalline and flexible Ti foil (as reported in our previous work,[5]). While this achievement represents an important step towards realization of bendable GaN-NW based devices on metal foils, the mechanism responsible for vertical NW growth remained unclear. In order to control the realization of vertically oriented GaN NW ensembles on polycrystalline metal foils, it is essential to uncover the underlying mechanism governing their direction of growth.

In this work, we investigate the effect of roughness, chemical composition, and crystallinity of the substrate surface on the orientation of self-assembled GaN NWs grown on polycrystalline Ti foils by plasma-assisted molecular beam epitaxy (PA-MBE). Regardless of the surface roughness of the as-received foil, we detect strong chemical reactions upon NW growth, which result in roughening of the substrate surface and the subsequent formation of randomly oriented NWs. Substrate nitridation preceding the NW growth is found to effectively diminish detrimental surface chemical reactions. On these nitridated Ti foils, we observe the formation of uniformly tilted NW ensembles within each individual grain of the polycrystalline substrate. Finally, we show that the GaN NWs grow vertically when the foil is covered by a thin amorphous oxide layer. This finding is ascribed to an interruption of the epitaxial relation with the underlying substrate.

2. Experimental

In this study, two different types of Ti foils are investigated as substrates for GaN NW growth; the first one is a 10×10 mm^2 large and 400 µm thick foil from MTI with a purity of 99.9%. The second one is a 25×25 mm^2 large and 127 µm thick foil from Alpha Aeser with a purity of 99.99%. In the following, we refer to these substrates as foils A and B, respectively. The foils have been investigated by atomic force microscopy (AFM), electron backscatter diffraction (EBSD), X-ray photoelectron spectroscopy (XPS), spectroscopic ellipsometry, and Raman spectroscopy. These have been examined both as-received and after a chemical treatment, consisting in either (i) a 30 min H_2 annealing at 700 °C in order to remove the native surface oxide, (ii) a high-temperature nitridation process, or (iii) a combination of these two surface treatments. The H_2 annealing is performed in a separate chamber interconnected with the PA-MBE system, wich serves for both substrate nitridation and subsequent growth of the GaN NWs. Nitridation is initiated by opening the N shutter and ramping up the substrate temperature from 100 to 1000 °C at a rate of 0.5 °C/s. After reaching 1000 °C, the foil is continuously

nitridated at this temperature for 20 minutes. The N flux during nitridation is the same one as that used for the growth of the GaN NWs, as specified below.

GaN NWs are grown both on the as-received foils and on foils subjected to surface treatment in a MBE system equipped with a radio-frequency N_2 plasma source and a solid-source effusion cell for Ga. In all experiments reported here, the Ga and N fluxes are 3.9×10^{14} and 8.5×10^{14} at s^{-1} cm^{-2}, respectively, with a total growth time of 4 hours. The substrate temperature during GaN growth, measured with a thermocouple attached to the substrate heater, is tuned in the range 740—780 °C in order to achieve ensembles of uncoalesced NWs. The GaN NW ensembles are inspected by scanning electron microscopy (SEM). A complete list of samples, including the ones with NW ensembles, is given in Table 1. As-received and surface treated foils of type A and B are labeled as A0, A1,... and B0, B1,..., respectively, while those with MBE-grown GaN NWs are labeled as S_{A0}, S_{A1},... and S_{B0}, S_{B1}. For the latter, the subscript A0, B0,... indicates the type of foil and surface treatment prior to NW growth.

Atomic force micrographs are recorded with a Bruker Dimension Edge microscope equipped with a Si tip and operated in peak force mode. EBSD analysis is performed with a ZEISS Ultra-55 microscope, while scanning electron micrographs are recorded in a Hitachi S-4800 SEM operated at 5 kV. XPS spectra are measured at normal and 60° off-normal emission in a Kratos Analytical AXIS Ultra DLD spectrometer using monochromated Al K_α X-rays. Spectroscopic ellipsometry is performed at a fixed incidence angle of 57° in a Sopra GES5E ellipsometer. Raman analysis is carried out in a Horiba/Joblin-Yvon Labrun HR Evolution system. For this analysis the Ti foils are optically excited at 2.62 eV (473 nm). The Raman signal is dispersed using a 1800 grooves/mm grating and detected with a liquid-N_2-cooled charge coupled device camera. These measurements are performed at room temperature in a backscattering geometry.

3. Results and discussion

3.1. Morphology and crystallinity of the as-received Ti foils

Atomic force microscopy is carried out to investigate the surface morphology of the as-received foils. The recorded micrograph of sample A0 [Fig. 1 (a)] shows a rather flat and homogeneous foil surface with a root mean square (RMS) roughness of 1.8 nm and the presence of scattered nm-sized particles. In contrast, sample B0 exhibits an uneven and inhomogeneous surface characterized by an RMS roughness of 6.3 nm and the presence of elongated voids with a lateral dimension of up to 1 µm [Fig. 1(b)].

Table 1. Summary of investigated samples and their corresponding surface treatment (i. e., H_2 annealing and nitridation). Samples prepared on foils A and B are labeled A0, A1,... and B0, B1,..., respectively. NW ensembles are labeled S_{A0}, S_{B0},...where the subscript A0, B0,...indicates the surface treatment of the foil prior to GaN growth. V and X indicate whether a certain surface treatment is carried out or not for a specific sample, respectively.

Sample	H_2 annealing	Nitridation
A0	✗	✗
B0	✗	✗
A1	✓	✗
B1	✓	✗
A2	✗	✓
B2	✗	✓
A3	✓	✓
B3	✓	✓
S_{A0}	✗	✗
S_{B0}	✗	✗
S_{A1}	✓	✗
S_{A2}	✗	✓
S_{B2}	✗	✓
S_{A3}	✓	✓

The size and orientation of the grains composing foils A and B are investigated by EBSD. Prior to the analysis, the foils are heated in a H_2 atmosphere to remove their surface native oxide, as explained in the experimental section. Subsequently, the foils are transferred to our analytial SEM to ve studied by EBSD. Surface orientation maps measured for samples A1 and B1 are shown in Figs. 1(c) and 1(d), respectively. Sample A1 is found to consist of large grains with sizes ranging from a few tens to a few hundred μm [Fig. 1(c)]. These grains seem to have no preferential orientation, as is apparent in

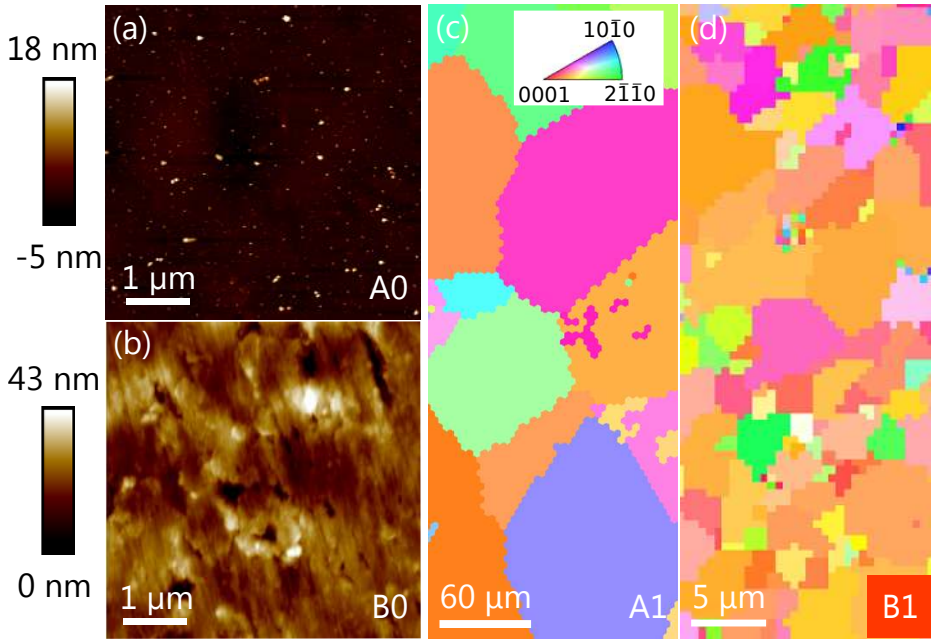

Figure 1. (a,b): 5×5 µm^2 atomic force micrographs of samples A0 and B0, respectively. EBSD orientation maps of samples A1 (c) and B1 (d). The legend in the upper right corner of (c) also applies to the map shown in (d).

the legend inserted in Fig. 1(c). In contrast, sample B1 features smaller grains with sizes ranging from sub-µm dimensions up to a few µm [Fig. 1(d)]. Moreover, a large fraction of the grains in this foil is found to exhibit a preferred orientation towards the $[11\bar{2}5]$ direction (orange color).

3.2. GaN nanowire growth

To investigate the impact of surface roughness and crystallinity of the starting substrate on the NW orientation, GaN NWs are grown directly on the as-received foils without any pre-growth treatment (samples S_{A0} and S_{B0}). Scanning electron micrographs showing the morphology and orientation of the self-assembled GaN NWs on the two types of Ti foils are displayed in Fig. 2. For sample S_{A0} [Fig. 2(a)], we observe a low density of NWs with an average diameter of approximately 50 nm and a mean length of approximately 1 µm. The NW areal density is significantly higher for sample S_{B0} [Fig. 2(b)]. The NWs grown on this sample also exhibit larger diameters and lengths of about 150 nm and 2 µm, respectively. In both cases, the NWs are found to grow with nearly random orientation on

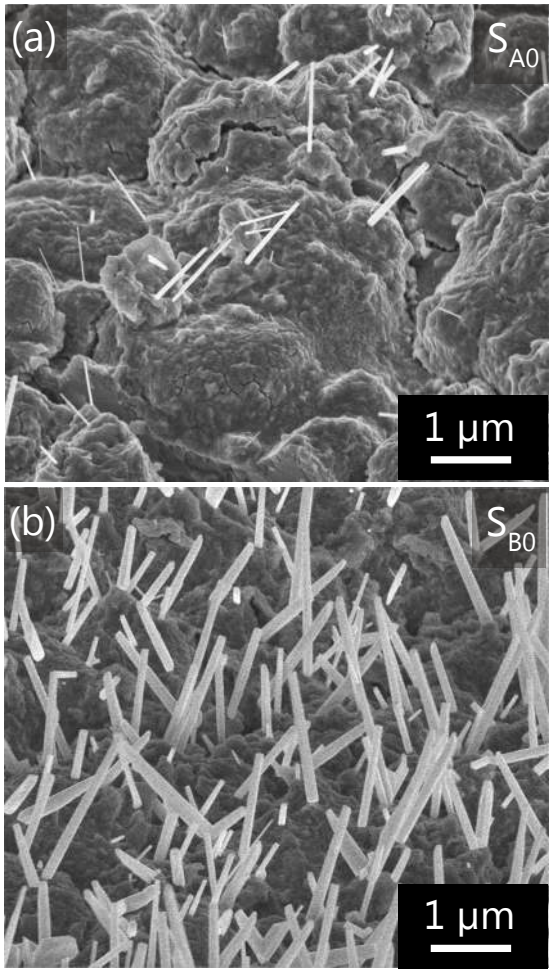

Figure 2. Bird's eye view scanning electron micrographs of samples S_{A0} and S_{B0} showing the grown GaN NW ensembless.

these Ti foils. The observed differences in NW morphology and density are tentatively attributed to differences in the actual substrate temperature during growth. Interestingly, despite a significant difference in the as-received surface morphology of foils A and B [Figs. 1(a) and 1(b)], the two substrates show enhanced and similar surface roughness after the NW growth. We attribute this roughening of the substrates to strong surface chemical reactions between the impinging elements and Ti, as well as with the native oxide. [23, 24] The nearly random NW orientation observed in Figs. 2 (a) and (b) is ascribed to the large surface roughness of the foils. This result indicates that, regardless

of the substrate crystallinity, an initially smooth surface is not sufficient to guarantee the vertical growth of GaN NWs on Ti foils. To this end, a surface pretreatment is needed to protect the substrate against these undesired chemical reactions.

In PA-MBE, a straightforward and natural approach for passivation of the Ti surface against chemical reactions is to form a protective surface layer of TiN prior to NW growth. [25] TiN also serves to form an ohmic contact with GaN [26] and can be readily formed by exposing the substrate surface to a N plasma in the PA-MBE system.[1, 25] In order to study the impact of substrate nitridation on the orientation of self-assembled GaN NWs grown on Ti foils, two samples are grown on foil A with (sample S_{A3}) and without (sample S_{A1}) a pre-growth nitridation step after annealing the substrate in a H_2 atmosphere to remove the native surface oxide.

Figures 3(a) and (b) show bird's eye view scanning electron micrographs of samples S_{A1} and S_{A3}, respectively. Both samples exhibit a rough surface, with a roughness comparable in magnitude to that of samples S_{A0} and S_{B0} in Fig. 2. However, the roughening of the substrate surface upon GaN NW growth show different characteristics for the two samples, which indicates the impact of the nitridation step. While both samples are rough on a macroscopic scale, sample S_{A3} exhibit smooth and inclined terrace-like areas which are totally absent in sample S_{A1}. This difference in surface morphology is found to strongly affect the orientation of the GaN NWs. In sample S_{A1} [Fig. 3(a)], the NWs exhibit a wide variety of tilt angles with respect to the substrate normal, as they do for NWs grown on as-received foils (cf. Fig. 2). A different result is found for sample S_{A3} [Fig. 3(b)]. In this sample, the vast majority of NWs assume one out of two preferred growth directions with respect to the substrate normal. Only a minor fraction of NWs grow at a different tilt angle. Based on these findings, we attribute the preferred growth of NWs in well-defined directions to their nucleation on the terrace-like substrate areas formed during nitridation. It is important to note that these preferred growth directions vary across the sample (not shown here). This observation can be explained by the polycrystalline nature of the foil, with grains with lateral dimensions from tens to a few hundred μm [see Fig. 1(c)]. Thus, for nitridated substrates the GaN NW orientation is not determined by the surface roughness, but by the crystallinity of the original foil.

The results obtained for the growth on the H_2-treated and nitridated foil are consistent with the findings reported by May et al. [6] who also observed uniformly tilted GaN NWs within the individual grains of Ti and Ta foils. However, these results are in sharp contrast to those reported in our previous paper, where vertically oriented GaN NWs were

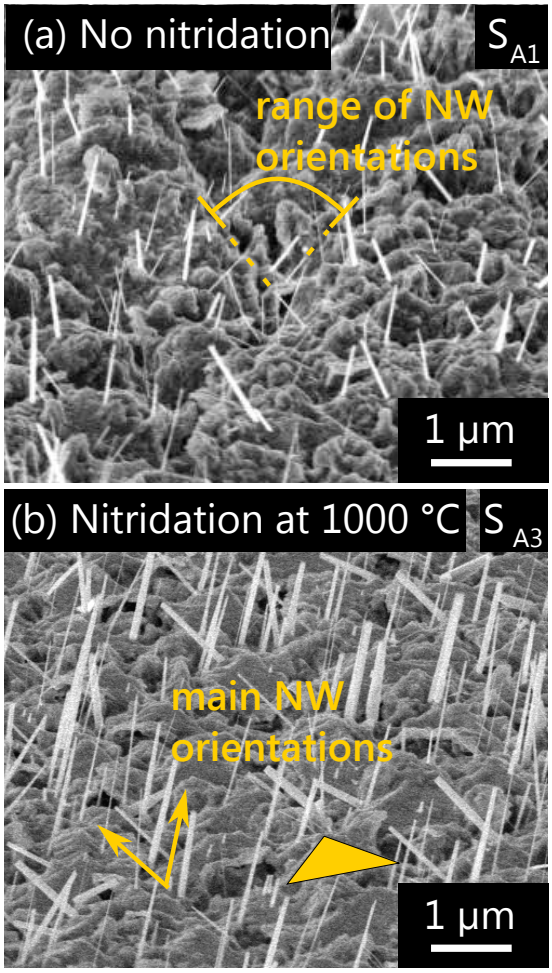

Figure 3. Bird's eye view scanning electron micrographs of samples S_{A1} (a) and S_{A3} (b). In (b) a terrace-like surface patch is indicated

achieved for growth on a nitridated Ti foil of type B.[5] To elucidate the underlying reason behind these apparently contradictory results, we also analyze the growth of GaN NWs on nitridated foils of the types A and B, omitting the H_2 substrate annealing step.

Figure 4 shows low- and high-magnification bird's eye view scanning electron micrographs of NW ensembles grown on nitridated but not H_2 annealed foils (samples S_{A2} and S_{B2}). The NWs in sample S_{A2} [Figs. 4(a) and 4(b)] show a locally uniform tilt angle with respect to the substrate normal (as in sample S_{A1} [Fig. 3(b)]), which changes across the foil. For sample S_{B2}, the result is much different. Despite the severe roughening of the

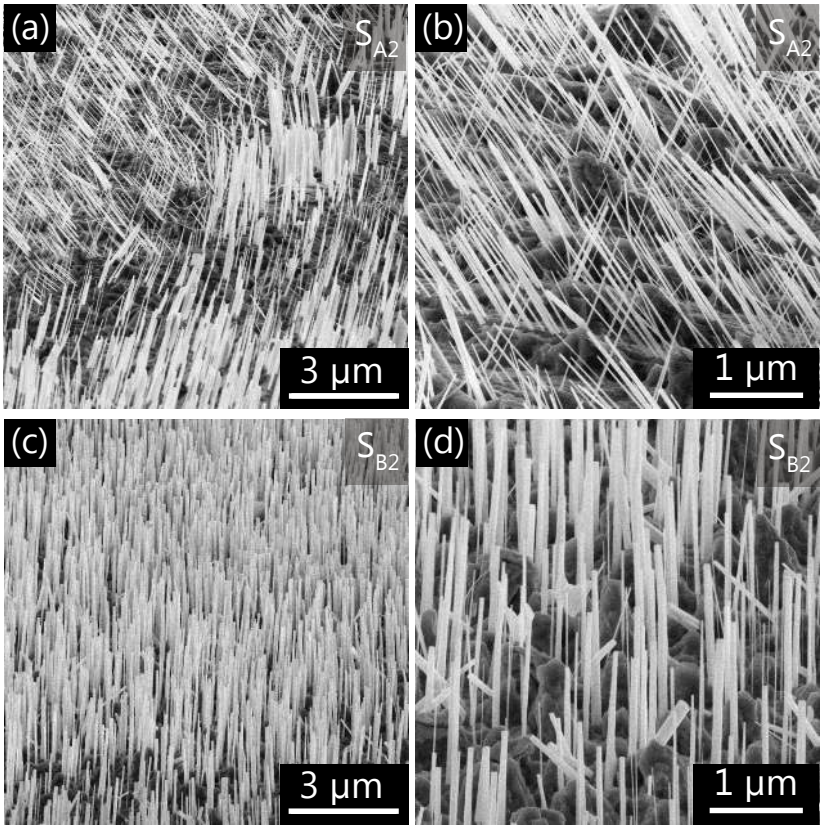

Figure 4. Low and high magnification bird's eye view scanning electron micrographs of samples S_{A2} and S_{B2}

initial substrate surface, the NWs grow vertically oriented all across the foil as reported in Ref. 5 and shown in Figs. 4(c) and 4(d). EBSD analysis of samples A3 and B3 (not shown here) show that the foils remain polycrystalline after the nitridation process. Therefore, the vertical orientation of the NWs in sample S_{B2} cannot be attributed to growth on a textured substrate which has recrystallized during the high-temperature nitridation step. In the following, we investigate whether the different results obtained for foils A and B are related to the structural and chemical properties of the native oxide present on the as-received substrates.

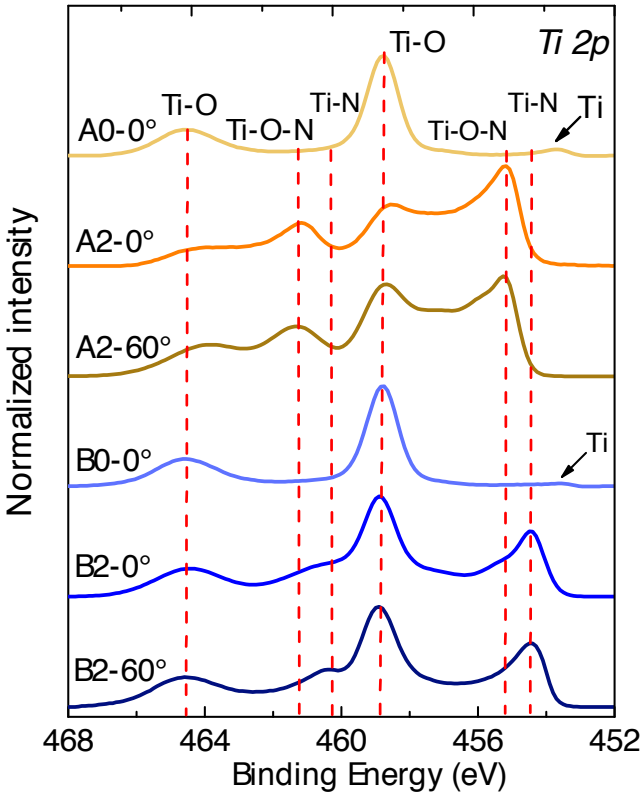

Figure 5. Ti 2p XPS spectra of samples A0, B0, A2 and B2. For the latter two samples, spectra measured at both normal and 60° off-normal emission are included. The spectra are normalized to the higher intensity peak and vertically shifted for clarity.

3.3. Impact of the native oxide layer on nanowire orientation

In order to examine the cause for the observed difference in NW orientation for samples S_{A2} and S_{B2}, the surface chemical states of the foils are investigated with XPS before and after nitridation. The XPS spectra of the Ti 2p core-levels, normalized to the peak of maximum intensity, are shown in Fig. 5. The spectra acquired from the as received foils are measured in normal emission (samples A0-0° and B0-0°) and show the spin-orbit split Ti $2p_{3/2}$ and Ti $2p_{1/2}$ core-level emission from the native surface TiO_2 at 458.8 and 464.5 eV binding energy (BE), respectively.[27] In addition, a low intensity but distinct Ti metal peak is present for both samples at 453.7 eV BE. After substrate nitridation, spectra of both foils (samples A2 and B2) are acquired in normal (A2-0° and B2-0°) as well as 60° off-normal emission (A2-60° and B2-60°), showing a set of new peaks centered at

455.2 and 461.2 eV BE for sample A2, and 454.5 and 460.3 eV BE for sample B2.

In agreement with previous work,[28, 29] the Ti $2p_{3/2}$ and Ti $2p_{1/2}$ peaks observed for sample A2 are attributed to the formation of Ti oxynitrides (TiO_xN_y), while those observed for sample B2 are attributed to the formation of TiN_x at the sample surface. Minor contributions to the Ti $2p_{3/2}$ and Ti $2p_{1/2}$ peaks of the specta of sample A2 at 455.9 and 457.9 eV BE, seen primarily in off-normal emission (spectrum A2-60°), are ascribed to surface TiO_xN_y with a reduced share of N. In sample B2 we also note high energy shoulders of the Ti $2p_{3/2}$ and Ti $2p_{1/2}$ peaks at 455.1 and 461.2 eV BE, respectively, which we attribute to the presence of TiO_xN_y. These findings indicate for foil of type A that nitridation carried out prior to NW growth results in the formation of TiO_xN_y on sample surface. In contrast, nitridation of B-type foil leads to formation of TiN_x, as previously reported for nitridated Ti films sputter-deposited on Al_2O_3[1], with a small volume fraction of TiO_xN_y. After nitridation, we still observe emission from Ti-O in both samples, suggesting that the native surface oxide partly survives this treatment. However, while the Ti-O-N peak is the more pronounced feature of the A2 spectra, the Ti-O emission at 458.8 eV BE is predominant in the B2 spectra. Thus, the native oxide layer of foil B appears to be more robust against nitridation than that of foil A. The comparison of the A2-0° and A2-60° spectra reveals a higher intensity ratio between the Ti-O and Ti-O-N related peaks for the spectrum acquired at 60° collection angle. TiO_2 thus appears to be more abundant in the topmost layer of the substrate. On the other hand, the intensity ratio between the Ti-O and Ti-N peaks is virtually independent of the emission angle. Therefore, we conclude that TiO_2 and TiN_x coexist (along with TiO_xN_y) at the surface of sample B2.

The difference in stability of the native surface oxide on foils A and B against plasma nitridation suggests that these oxides are structurally different. Thus, we also examin these surface oxides by spectroscopic ellipsometry and Raman spectroscopy. Figure 6 (a) and (b) show the real (ε_1) and imaginary parts (ε_2) of the pseudodielectric function obtained by spectroscopic ellipsometry for the as-received Ti foils (A0 and B0). For comparison, we have also included the real and imaginary parts of the dielectric function of bulk Ti. The spectra of both foils are found to vary slightly across the surface (not shown here), suggesting the presence of a non-uniform surface oxide. Attempts to fit the spectra from sample A0 assuming a rutile, anatase or amorphous TiO_2 layer on top of bulk Ti were unsuccesfull, an indication the A0 native oxide has no well-defined structural order. In contrast, above 2.5 eV the spectra measured on sample B0 can be reasonably fitted assuming a 1 nm thick amorphous or anatase TiO_2 layer on bilk Ti (we cannot

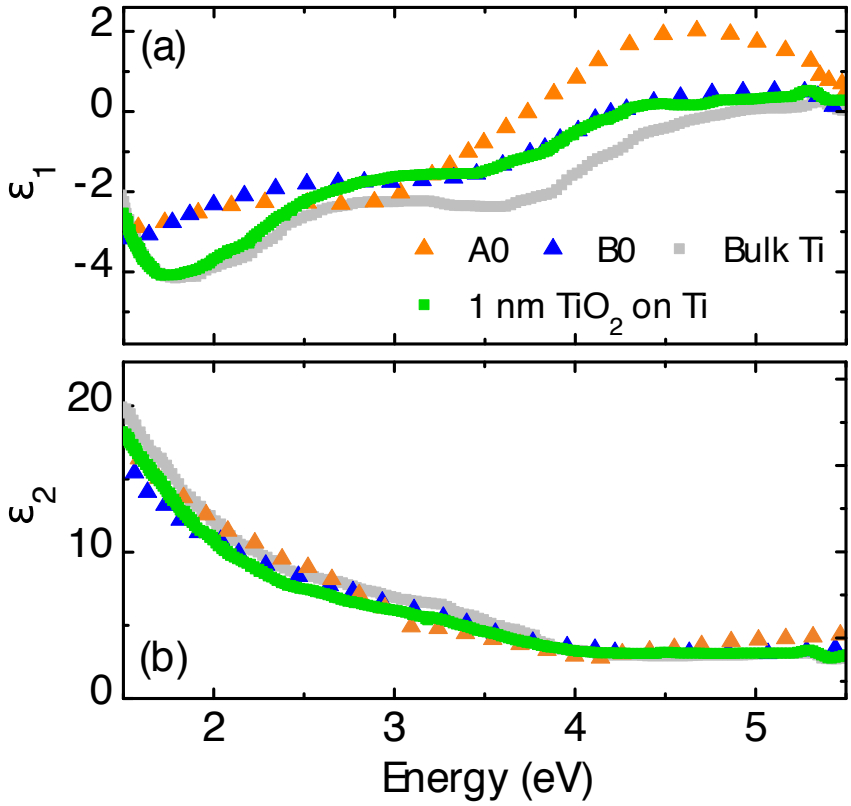

Figure 6. Real (a) and imaginary (b) parts of the pseudodielectric function obtained by spectroscopic ellipsometry for the as-received Ti foils (A0 and B0). The real and imaginary parts of the dielectric function for bulk Ti are also included for comparison. The green triangles represent a fit to the experimental data from sample B0, assuming an anatase or amorphous TiO_2 surface layer on bulk Ti. The thickness of the TiO_2 layer derived from this fit is 1 nm.

distinguish between amorphous and anatase TiO_2 by optical ellipsometry because of their similar electronic structure[30]), as seen from the corresponding fit in Fig. 6.

In order to gain further insight into the crystal phase of the native Ti surface oxide on the as-received foils A and B, we analyze the samples by Raman spectroscopy. Representative Raman spectra of foils A0 and B0 between 125 and 700 cm^{-1} (i. e., the region of optical phonons for TiO_2) are shown in Fig. 7. Both spectra differ significantly from those of anatase and rutile TiO_2, for which a strong phonon line in the range between 610 to 640 cm^{-1} is characteristic.[31] Instead, the spectrum of sample A0 is dominated

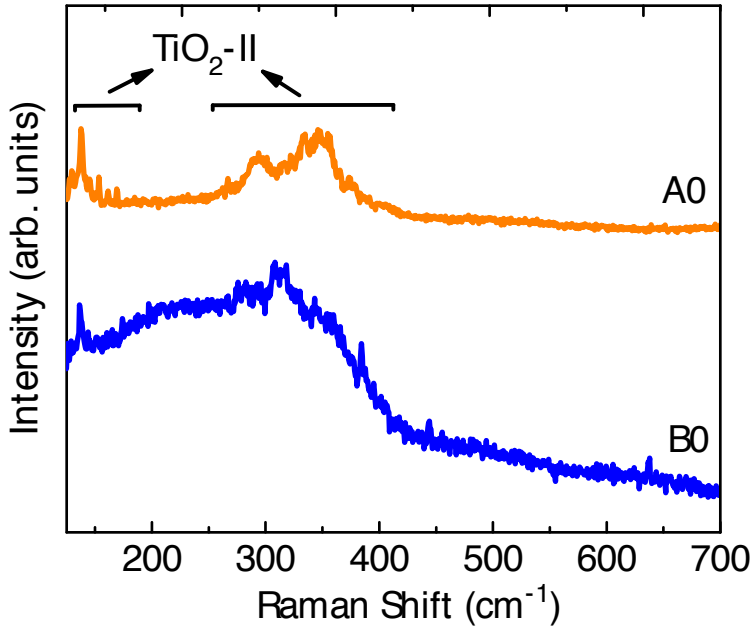

Figure 7. Room temperature Raman spectra of the as-received foils A0 and B0. The bars indicate the position of peaks compatible with the presence of surface TiO_2-II. The two spectra are vertically shifted for clarity.

by Raman features around 150 cm^{-1} and in the range between 250 and 400 cm^{-1}, resembling the spectra for the unusual TiO_2-II crystalline phase reported by Sekiya et al. after applying to the substrate a hydrostatic pressure above 4 GPa. [32] The observation of this phase, which was attributed to a pressure-induced irreversible transition from the anatase phase,[32] could result from the fabrication process of this foil (the fabrication of metal foils typically involves high-pressure rolling). The Raman spectrum of sample B0 is dominated by a broad band characteristic of amorphous TiO_2.[33, 34] Superimposed on this band, we also observe more sharp Raman features around 150 cm^{-1} and in the range between 300 and 400 cm^{-1}. These Raman features, with a lower intensity, are again compatible with a small fraction of the TiO_2-II phase. The frequency shifts and variation in relative intensities of the Raman features with respect to those observed in sample A0 are tentatively ascribed to the difference in pressure applied to the foils during their respective fabrication processes.[32]

Dissimilarities of the native surface oxide on the as-received foils provide a natural explanation for the different orientation of the GaN NWs grown on foils A and B,

respectively. The native oxide on foil A has characteristics consistent with a crystalline TiO_2-II layer, which is transformed into TiO_xN_y upon nitridation. On this substrate, GaN NWs grow epitaxially and thus uniformly tilted within the individual grains of the polycrystalline Ti foil. In the case of foil B, the native oxide layer is mainly amorphous and more robust against nitridation. Hence, the formation of well-aligned and vertically oriented GaN NWs on this substrate can be explained by their nucleation on amorphous TiO_2 as well as on amorphous TiN_x and TiO_xN_y, which prevent the transfering of the epitaxial information from underlying polycrystalline substrate.35

4. Summary and conclusions

We have shown that the orientation of self-assembled GaN NWs on Ti foil from different vendors depends critically on both the chemical composition and the crystallinity of the native surface oxide. Regardless of the initial morphology of the as-received foil, we find severe roughening of the substrate surface as a result of the chemical reactions occurring between the impinging elements and Ti. These chemical reactions and the concomitant roughness lead to the formation of randomly oriented GaN NWs. We find out that a surface plasma nitridation prior to GaN NW growth reduces the roughening of the surface by transformation of the topmost layers into more stable compounds, i.e., TiN_x and TiO_xN_y. On nitridated foils, GaN NWs have been found to be well aligned, but their specific orientation depends critically on the crystalline properties of the surface oxide after nitridation. For the investigated foils, we have found that the native oxide layer is either crystalline or predominantly amorphous. When the native oxide is crystalline, GaN NWs grow homogeneously tilted within the individual grains of the substrate. In contrast, the presence of an amorphous surface oxide prevents epitaxial growth. The NWs then grow vertically oriented all across the substrate. This result is consistent with those reported in Refs. 36 and 35, where ensembles of vertically orientated GaN NWs were grown on amorphous Si_xO_y and Al_xO_y layers deposited on crystalline Si substrates.

This study thus demonstrates that a thermally stable amorphous layer of TiO_2 or TiO_xN_y serve as a suitable interlayer for the growth of vertically oriented GaN NWs on Ti foils. This finding may be exploited for the fabrication of GaN NW-based bendable devices without relying on lift-off or substrate transfer techniques. Of course, the successful direct fabrication of efficient bendable electronic and photonic devices from NWs grown on metal foils will strongly depend on the resistance introduced by TiO_2/TiO_xN_y layer. Amorphous TiO_2 is an electrical insulator with a high electrical

resistivity. It follows that effective carrier injection from the Ti foil into the GaN NWs could only be achieved in the presence of extended defects (as in the case of GaN NW-based LEDs fabricated on AlN buffered Si) [37] or by electron tunneling, an effect that strongly depends on the thickness of the oxide layer. For the fabrication of devices, it will be thus essential to control the formation of the surface oxide layer. Suitable control could possibly be achieved, for example, by an anodization processes[38]. An alternative strategy for vertically oriented NWs on a Ti foil, without sacrificing the benefit of a highly electrically conductive substrate, would be the introduction of a conducting and amorphous interlayer, such as a TiO_xN_y layer fabricated under specific conditions.[39]

Finally, our findings could be extended to the formation of self-assembled and vertically oriented NWs of different semiconductors (e.g. ZnO) on other types of metal foils provided that the surface is passivated against detrimental chemical reactions and covered by a thermally stable amorphous layer.

Acknowledgments

We thank Carsten Stemmler, Michael Höricke, and Hans-Peter Schönherr for their dedicated maintenance of the MBE system, Anne-Kathrin Bluhm for her support with the scanning electron microscope, and XXX for critical reading of the manuscript. Financial support of this work by the Leibniz-Gemeinschaft under Grant SAW-2013-PDI-2 is gratefully acknowledged.

References

[1] Wölz M, Hauswald C, Flissikowski T, Gotschke T, Fernández-Garrido S, Brandt O, Grahn H T, Geelhaar L and Riechert H 2015 *Nano Lett.* **15** 3743–3747

[2] Yang Z, Wang M, Shukla S, Zhu Y, Deng J, Ge H, Wang X and Xiong Q 2015 *Scientific Reports* **5** 11377

[3] Sarwar A G, Carnevale S D, Yang F, Kent T F, Jamison J J, McComb D W and Myers R C 2015 *Small* **11** 5402–5408

[4] Zhao C, Ng T K, Wei N, Prabaswara A, Alias M S, Janjua B, Shen C and Ooi B S 2016 *Nano Letters* **16** 1056–1063

[5] Calabrese G, Corfdir P, Gao G, Pfüller C, Trampert A, Brandt O, Geelhaar L and Fernández-Garrido S 2016 *Applied Physics Letters* **108** 202101

[6] May B J, Sarwar A T M G and Myers R C 2016 *Applied Physics Letters* **108** 141103

[7] Zhao C, Ng T K, ElAfandy R T, Prabaswara A, Consiglio G B, Ajia I A, Roqan I S, Janjua B, Shen C, Eid J, Alyamani A Y, El-Desouki M M and Ooi B S 2016 *Nano Letters* **16** 46164623

[8] Janjua B, Ng T K, Zhao C, Prabaswara A, Consiglio G B, Priante D, Shen C, Elafandy R T, Anjum D H, Alhamoud A A, Alatawi A A, Yang Y, Alyamani A Y, El-Desouki M M and Ooi B S 2016 *ACS Photonics* **3** 2089–2095

[9] Janjua B, Ng T K, Zhao C, Oubei H M, Shen C, Prabaswara A, Alias M S, Alhamoud A A, Alatawi A A, Albadri A M, Alyamani A Y, El-Desouki M M and Ooi B S 2016 *Optics Express* **24** 19228

[10] Treeck v D, Calabrese G, Goertz J, Kaganer V, Brandt O, Fernández-Garrido S and Geelhaar L 2017 *Manuscript submitted for publication*

[11] Tomioka K, Motohisa J, Hara S and Fukui T 2008 *Nano letters* **8** 3475–80

[12] Urban A, Malindretos J, Klein-Wiele J H, Simon P and Rizzi A 2013 *New Journal of Physics* **15** 053045

[13] Richards B T, Gaskey B, Levin B D a, Whitham K, Muller D and Hanrath T 2014 *Journal of Materials Chemistry C* **2** 1869

[14] Lopez O E, Tucker A L, Singh K R, Mamer S B, Sadoqi M and Xu H 2014 *Superlattices and Microstructures* **75** 358–370

[15] Nandhyala S, Haji-Sheikh M, Kocanda M and Rajashankar S 2014 *Proceedings of the 8th International Conference on Sensing Technology* 68–72

[16] DeJarld M, Teran A, Luengo-Kovac M, Yan L, Moon E S, Beck S, Guillen C, Sih V, Phillips J and Milunchick J M 2016 *Nanotechnology* **27** 495605

[17] Tsakalakos L, Balch J, Fronheiser J, Korevaar B A, Sulima O and Rand J 2007 *App. Phys. Lett.* **91** 233117

[18] Fan Z, Razavi H, Do J w, Moriwaki A, Ergen O, Chueh Y L, Leu P W, Ho J C, Takahashi T, Reichertz L A, Neale S, Yu K, Wu M, Ager J W and Javey A 2009 *Nature Materials* **8** 648–653

[19] Oulton R F, Sorger V J, Zentgraf T, Ma R M, Gladden C, Dai L, Bartal G and Zhang X 2009 *Nature* **461** 629–632

[20] Gu Z, Paranthaman M P, Xu J and Pan Z W 2009 *ACS Nano* **3** 273–278

[21] Rakesh Kumar R, Narasimha Rao K and Phani A R 2011 *Appl. Nanoscience* **1** 211–217

[22] Li H, Zhao G, Wang L, Chen Z and Yang S 2016 *Nanomaterials* **6** 195

[23] Bauer E G, Dodson B W, Ehrlich D J, Feldman L C, Flynn C P, Geis M W, Harbison J P, Matyi R J, Peercy P S, Petroff P M, Phillips J M, Stringfellow G B and Zangwill A 1990 *J. Mater. Res.* **5** 852–894

[24] Palmstrøm C J 1995 *Ann. Rev. Mater. Sci.* **25** 389–415

[25] Bengoechea-Encabo A, Barbagini F, Fernández-Garrido S, Grandal J, Ristić J, Sanchez-García M A, Calleja E, Jahn U, Luna E and Trampert A 2011 *Journal of Crystal Growth* **325** 89–92

[26] Ruvimov S, Liliental-Weber Z, Washburn J, Duxstad K J, Haller E E, Fan Z F, Mohammad S N, Kim W, Botchkarev A E and Morkoç H 1996 *Appl. Phys. Lett.* **69** 1556

[27] Lu G, Bernasek S L and Schwartz J 2000 *Surface Science* **458** 80–90

[28] Milošev I, Strehblow H H, Navinšek B and Metikoš-Huković M 1995 *Surface and Interface Analysis* **23** 529–539

[29] Cheng Y and Zheng Y 2007 *Surface and Coatings Technology* **201** 6869–6873

[30] Prasai B, Cai B, Underwood M K, Lewis J P and Drabold D A 2012 *Journal of Materials Science* **47** 7515–7521

[31] Frank O, Zukalova M, Laskova B, Kürti J, Koltai J and Kavan L 2012 *Physical Chemistry Chemical Physics* **14** 14567

[32] Sekiya T, Ohta S, Kamei S, Hanakawa M and Kurita S 2001 *Journal of Physics and Chemistry of Solids* **62** 717–721

[33] Bradley J D B, Evans C C, Choy J T, Reshef O, Deotare P B, Parsy F, Phillips K C, Lončar M and Mazur E 2012 *Optics Express* **20** 23821–23831

[34] Lee C M and Choi J 2016 *Optical Materials Express* **6** 3594–3608

[35] Sobanska M, Wierzbicka A, Klosek K, Borysiuk J, Tchutchulashvili G, Gieraltowska S and Zytkiewicz Z 2014 *Journal of Crystal Growth* **401** 657–660

[36] Stoica T, Sutter E, Meijers R J, Debnath R K, Calarco R, Lüth H and Grützmacher D 2008 *Small* **4** 751–754

[37] Musolino M, Tahraoui A, Fernández-Garrido S, Brandt O, Trampert A, Geelhaar L and Riechert H 2015 *Nanotechnology* **26** 085605

[38] Yamamoto D, Iida T, Kuroda K, Ichino R, Okido M and Seki A 2012 *Materials Transactions* **53** 508–512

[39] Chen C H, Cheng C E, Hsu C C, Chang M N, Shiu H W and Chien F S S 2012 *Journal of Physics D: Applied Physics* **45** 215307